IOSR Journal of Environmental Science, Toxicology and Food Technology (IOSR-JESTFT)
e-ISSN: 2319-2402, p- ISSN: 2319-2399.Volume 20, Issue 8 Ser. II (August 2026), PP 01-10
www.iosrjournals.org

Mining-Influenced Landscape Reconfiguration in Part of Jos South L.G.A., Plateau State, Nigeria: Landcover Transitions, Surface-Exposure Signals and Persistent Mining Pond Corridors, 2000 – 2026.

Dare Peter Mayowa[1a], Dauda Dung Dung[2b], Jibril Mohammed[3c], Inusa Titus[4d], Chindo I.Y.[5e].

[1] Department of Environmental Node, Faculty of Sustainable Procurement Environmental and Social Standards Enhancement Centre of Excellence, Abubakar Tafawa Balewa University, P.M.B. 0248, Bauchi, Nigeria.
[2] National Centre for Remote Sensing, Jos, Nigeria.
[3] Department of Chemical Engineering, Faculty of Engineering, Abubakar Tafawa Balewa University, P.M.B. 0248, Bauchi, Nigeria.
[4] Department of Environmental Node, Faculty of Sustainable Procurement Environmental and Social Standards Enhancement Centre of Excellence, Abubakar Tafawa Balewa University, P.M.B. 0248, Bauchi, Nigeria.
[5] Department of Chemistry, Faculty of Science, Abubakar Tafawa Balewa University, P.M.B. 0248, Bauchi, Nigeria.

Abstract:
Mining landscapes are often interpreted from net land cover gains and losses, yet such summaries can conceal substantial exchanges among cultivated land, exposed substrates, settlements, vegetation and water filled excavations. This study examined landscape reconfiguration across a 335.66Km² mapped portion of Jos South Local Government Area (L.G.A.) Plateau State, Nigeria, between 2000 and 2026. Landsat 7 ETM+ (2000), Landsat 8 OLI/TIRS (2013) and Landsat 9 OLI 2/TIRS 2 (2026) imagery were classified into six land cover classes and analysed using post classification change detection and pixel based transition matrices. Normalised Difference Vegetation Index (NDVI), Bare Soil Index (BSI) and Normalised Difference Water Index (NDWI) were integrated with mapped mining locations, mining ponds, field observations and GPS evidence to characterise vegetation response, surface exposure and persistent wetness patterns. Built up land increased from 19.00Km² in 2000 to 78.52Km² in 2026, representing a 313.25% increase, while farmland declined from 203.00Km² to 135.86Km², a 33.07% reduction. Only 50.35% of the landscape retained its original mapped class over the study period. The dominant transitions were farmland to rock outcrop or exposed rocky substrate (47.99Km²) and farmland to Built-Up land (42.73Km²), demonstrating substantial competition for productive land. Forty six mining locations were identified, with notable clusters in the eastern, central and western sectors. Spatial analysis of the spectral indices showed stronger vegetation responses in parts of the western and north western areas, persistent exposed surface signals around mining and settlement corridors, and recurrent positive NDWI signatures within the western and south western mining pond belt. The findings indicate that Jos South is undergoing heterogeneous, multi driver landscape reconfiguration in which mining legacies interact with urban expansion, cultivation, secondary vegetation development and hydrological modification. The study demonstrates that transition based and feature specific monitoring provides a more defensible basis for interpreting mining influenced landscape change than reliance on endpoint land cover totals alone.
Key Word*: Artisanal and Small-Scale Mining; Landcover Transition; Landsat; Mining Ponds; NDVI; Bare Soil Index; NDWI.*

Date of Submission: 13-08-2026 Date of Acceptance: 27-08-2026

I. Introduction

Artisanal and small-scale mining (ASM) can transform land far beyond the immediate excavation footprint. Vegetation clearance, removal of soil, exposure of bedrock and mine spoil, creation of access routes and water-filled pits can occur together with settlement growth, cultivation and infrastructure expansion. Consequently, mining landscapes often develop as heterogeneous mosaics rather than as a simple sequence from vegetation to bare ground. Recent reviews of remote sensing applications to ASM emphasise the need to combine repeated Earth observation with field or locally grounded evidence because informal mining footprints can be small, spectrally complex and spatially dynamic (Nursamsi et al., 2024). Evidence from West African mining districts similarly shows that mining, settlement and agricultural change frequently overlap, making attribution difficult when analysis is based only on class totals (Gbedzi et al., 2022; Bansah et al., 2024; Mensah et al., 2025).

The Jos Plateau provides a long-established mining landscape in which this problem is especially relevant. Tin and columbite extraction has operated for more than a century, leaving active workings, abandoned excavation pits, mine spoil and artificial ponds interspersed with rapidly expanding peri-urban settlements. Previous work in Jos South has identified mining-degraded sites and demonstrated the utility of geospatial methods for locating disturbance (Bala et al., 2021). Studies around Bukuru linked tin mining with vegetation disturbance and Landcover change (Musa & Jiya, 2011; Ndace & Danladi, 2012), while later analysis reported localised vegetation improvement alongside continuing pressure from mining and urbanisation (Ogunro & Owolabi, 2023). These mixed trajectories make it unsafe to equate higher vegetation response or lower mapped bare-soil area with ecological recovery without examining what the disturbed land became.

Multi-date Landcover maps provide a first description of landscape composition, but post-classification transition matrices reveal the origin and destination of individual changes. This distinction is important in a mining environment because a location mapped initially as farmland or bare surface may later be represented as exposed rocky substrate, built-up land, secondary vegetation or water. Transition analysis can therefore separate net change from gross exchange and persistence, while spectral indices provide independent spatial evidence of vegetation, surface exposure and water/moisture conditions. Intensity-analysis research further demonstrates the value of examining the amount and direction of categorical change rather than relying exclusively on net differences (Aldwaik & Pontius, 2012).

The novelty of this paper is therefore not the use of Landsat classification alone. It lies in integrating a full-period pixel transition matrix with mapped mining locations, exposed-surface signals and recurrent mining-pond corridors to distinguish persistent disturbance from apparent recovery. The study deliberately uses the term mining-influenced rather than mining-induced because urbanisation, roads, cultivation and natural or secondary vegetation dynamics can produce similar spectral and Landcover responses. Three questions guide the analysis: (1) how did the principal Landcover Classes change between 2000, 2013 and 2026; (2) which full-period transitions and persistence patterns dominated landscape reconfiguration; and (3) how do mapped mining locations, surface-exposure signals and recurrent pond/ wetness corridors modify interpretation of the class-level changes? (10)

II. Material And Methods

2.1 Study Area and Analytical Extent

The study covers a mapped portion of Jos South Local Government Area in Plateau State, north-central Nigeria, approximately between 9° 45′ and 9° 55′ N and 8° 45′ and 8° 58′ E. The highland landscape contains undulating terrain, rocky outcrops, Guinea Savanna vegetation, cultivated land, dense peri-urban settlement and an extensive legacy of tin-field excavation. Metropolitan expansion along the Jos-Bukuru axis adds substantial non-mining pressure on land. The common raster extent used for the temporal analysis is 335.66Km². Because the mapped polygon represents part of Jos South rather than a verified full administrative boundary, all area estimates and conclusions in this paper refer to the mapped analytical extent.

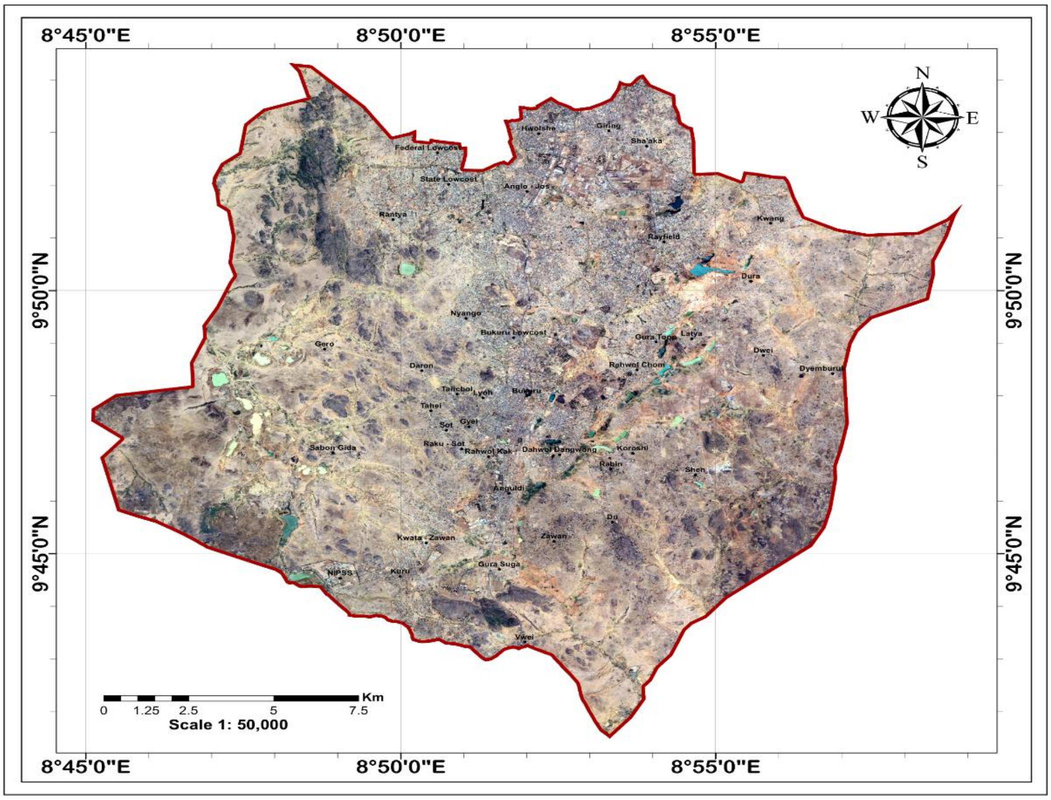

Figure 1. Satellite Image of Part of Jos South L.G.A. Plateau State.

2.2 Satellite Data and Temporal Design

Three Landsat imageries were analysed: Landsat 7 ETM+ for 2000, Landsat 8 OLI/ TIRS for 2013 and Landsat 9 OLI-2/TIRS-2 for 2026. The dates divide the 26-year period into two approximately equal 13-year intervals and provide a long-term baseline, an intermediate observation and a current endpoint. Landsat was selected because its 30m multispectral archive provides a consistent spatial framework for long-term land monitoring. The project utilized UTM Zone 32N (EPSG: 32632), 30m cells, identical dimensions and identical spatial extent. This alignment is essential for pixel-by-pixel post-classification comparison.

2.3 Image Preprocessing and Cross-Sensor Comparability

The documented preprocessing workflow comprised band preparation, geometric alignment to the common coordinate system, clipping to the analytical boundary, cloud/shadow screening where required and image enhancement for interpretation. Google Earth imagery, field observations and GPS evidence were used as ancillary information. For a submission-grade reproducible workflow, the final manuscript should state the exact product level and radiometric/ atmospheric correction applied to each scene. Where possible, archived USGS Collection 2 Level-2 surface-reflectance products should be used or confirmed because atmospheric correction improves temporal comparison of surface conditions. Regardless of product level, all three scenes must be seasonally comparable and quality-screened before direct comparison of index distributions.

Cross-sensor comparisons were interpreted conservatively. Landsat 7 ETM+, Landsat 8 OLI and Landsat 9 OLI-2 have related but non-identical spectral response functions. Accordingly, this study does not treat changes in a single extreme NDVI, BSI or NDWI pixel as a direct estimate of landscape-wide ecological change. The indices are used primarily to identify spatial correspondence among vegetation response, exposed surfaces, ponded water and mapped mining/settlement corridors. Class-transition results, which are based on the categorical maps aligned to the same 30 m grid, provide the primary evidence of landscape reconfiguration.

2.4 Landcover Classification and Operational Class Definitions

Supervised classification was used to generate six classes for each benchmark year: built-up area, farmland, vegetation, waterbody, bare surface and rock outcrop. Training samples were informed by spectral characteristics, visual interpretation, field knowledge and high-resolution reference imagery. The same final class scheme was retained across all years so that the maps could be compared directly. The operational class definitions used in the revised interpretation are shown in Table 1. Particular attention is given to the distinction between bare surface and rock outcrop because both may occur in mining and construction environments and can display overlapping spectral behaviour.

Table 1. Operational Interpretation of the Six Mapped Landcover Classes.

Class	Operational Interpretation
Built-Up Area	Buildings, dense settlement, roads and other developed or strongly impervious surfaces that were mapped as the built-up class.
Farmland	Cultivated fields, prepared agricultural land and agricultural mosaics mapped as farmland at the benchmark date.
Vegetation	Relatively continuous natural, secondary or regenerating vegetation distinct from cultivated farmland.
Waterbody	Open surface water, including natural/managed water features and water-filled excavation pits where mapped as water.
Bare Surface	Predominantly unconsolidated exposed soil, mine spoil, cleared ground or other sparsely vegetated surfaces not mapped as consolidated rock.
Rock Outcrop	Exposed consolidated rocky substrate and strongly rock-dominated surfaces, including mining-revealed rocky ground where it was separable from bare soil.

2.5 Accuracy Assessment and Classification Uncertainty

An independent accuracy-assessment design has been prepared for each classified map. Fifty stratified random validation points were generated within each of the six mapped classes, giving 300 points per year and 900 points across the three benchmark maps. Each point contains its geographic coordinates and mapped class and has been exported for independent interpretation against date-appropriate high-resolution imagery and, for the recent period, field evidence where available. The classified map itself is not used as the reference source. This design is consistent with the principle that map accuracy should be evaluated with reference information that is independent and more reliable than the map being assessed (Olofsson et al., 2014).

For each year, the completed reference labels should be used to construct a confusion matrix and report overall accuracy, class-specific user's accuracy and producer's accuracy, together with uncertainty estimates appropriate to the stratified sampling design. Kappa may be reported only as a secondary legacy statistic; quantity and allocation disagreement or the complete error matrix are more directly interpretable for Landcover comparison (Pontius & Millones, 2011). Because independent reference labels have not yet been entered into the available validation workbook, numerical accuracy values are not reported in this revision. Consequently, all transition quantities should be regarded as conditional on the final classification validation.

2.6 Post-Classification Change Detection and Transition Diagnostics

Post-classification change detection was performed by pixel-by-pixel cross-tabulation of the aligned classified rasters. With a 30 m cell size, each pixel represents 900 m² or 0.0009Km². Transition matrices were calculated for 2000-2013, 2013-2026 and the full period 2000-2026. The full-period matrix is presented in the main paper because it directly identifies the origin and destination of long-term changes, while the interval matrices can be retained as supplementary material. Row totals represent the 2000 class areas and column totals represent the 2026 class areas.

To distinguish persistence from exchange, the diagonal of the matrix was summed to estimate unchanged area. For each class, gross loss was calculated as the row total minus the diagonal cell; gross gain as the column total minus the diagonal cell; and net change as gross gain minus gross loss. These diagnostics prevent a small net change from being misread as stability when large reciprocal exchanges occurred. This is particularly important for rock outcrop, farmland and water, where similar endpoint totals can conceal substantial turnover.

2.7 Spectral Indices and Surface-Exposure Evidence

Three spectral indices were used as complementary spatial indicators. NDVI was calculated as (NIR - Red)/(NIR + Red) to characterise vegetation response. The Bare Soil Index (BSI) was calculated as [(SWIR1 + Red) - (NIR + Blue)]/[(SWIR1 + Red) + (NIR + Blue)] to emphasise exposed soil, rock, mine spoil and other sparsely vegetated surfaces. NDWI was calculated as (Green - NIR)/(Green + NIR) to enhance open-water and moisture signatures. Band equivalents were selected for each Landsat sensor according to the relevant visible, NIR and SWIR1 wavelengths.

Index minima and maxima are retained only as descriptive spectral extremes and not as estimates of mean condition or affected area. No percentage change in the maximum index value is interpreted as a percentage change in land condition. Likewise, a low BSI value inside a mining zone is not automatically treated as recovery because flooded pits, moist surfaces or vegetation can suppress the index while exposed spoil and banks remain nearby. A more rigorous future extension would classify all index rasters with common, independently validated thresholds and calculate area-based distributions; such threshold rasters were not available in the current manuscript package.

2.8 Mining-Site Mapping and Definition of Persistent Mining-Pond Corridors

The GIS inventory contained 46 mapped mining locations. In the original map these were labelled “hotspots”; however, no Getis-Ord Gi*, Local Moran’s I, kernel-density significance test or other inferential hotspot statistic is documented. The revised manuscript therefore refers to them as mapped mining locations, mining-site clusters or mining corridors rather than statistical hotspots. Their interpretation was based on the spatial concentration of known mining sites, disturbed surfaces, mapped ponds, field/GPS evidence and surrounding settlement/drainage features.

Mining-pond persistence is defined here at corridor scale rather than as the uninterrupted lifespan of every individual pond. A persistent mining-pond corridor is an area where mapped mining ponds and recurrent positive NDWI/wetness signatures occupy the same broad mining-drainage zone at the 2000, 2013 and 2026 benchmark dates. This definition is intentionally conservative because three snapshots cannot establish annual continuity, and pond expression can vary with rainfall, season, water depth, turbidity and vegetation. The analysis therefore supports spatial persistence of ponded mining landscapes, not a precise survival duration for each excavation.

2.9 Attribution Framework

The paper does not assign every transition to mining. A mining-influenced interpretation is supported only where several lines of spatial evidence are concordant: mapped mining locations or pond clusters, exposed-surface or wetness signatures, known mining corridors, and a transition pathway compatible with excavation or post-mining reworking. Built-up expansion, roads, cultivation and secondary vegetation are treated as competing or interacting drivers. This spatial-concordance framework is an attribution constraint rather than a causal estimator; without a formal counterfactual or mining/non-mining control model, the results identify plausible mining influence but do not quantify the fraction of each transition caused by mining.

III. Result

3.1 Landcover Composition and Long-Term Reconfiguration

Farmland remained the largest mapped class in all three benchmark years, but its trajectory changed markedly after 2013. It increased from 203.00Km² in 2000 to 224.71Km² in 2013 before contracting to 135.86Km² in 2026. Across the full period, farmland therefore lost 67.14Km², equivalent to 33.07% of its 2000 extent. Built-up land moved in the opposite direction, increasing from 19.00 to 78.52Km², a gain of 59.52Km² or 313.25%. The strongest reconfiguration occurred during 2013-2026, when built-up land gained 45.74Km² and farmland lost 88.86Km².

Table 2. Landcover Extent and Net Change Across the Three Benchmark Years.

Class	2000 Area (Km²)	2013 Area (Km²)	2026 Area (Km²)	Net Change (Km²)	Change (%)
Built-Up area	19.00	32.78	78.52	+59.52	+313.25
Farmland	203.00	224.71	135.86	-67.14	-33.07
Vegetation	8.84	17.28	17.75	+8.92	+100.90
Waterbody	4.43	6.02	4.70	+0.27	+5.99
Bare surface	6.11	2.45	2.27	-3.84	-62.88
Rock outcrop	94.29	52.42	96.57	+2.28	+2.42

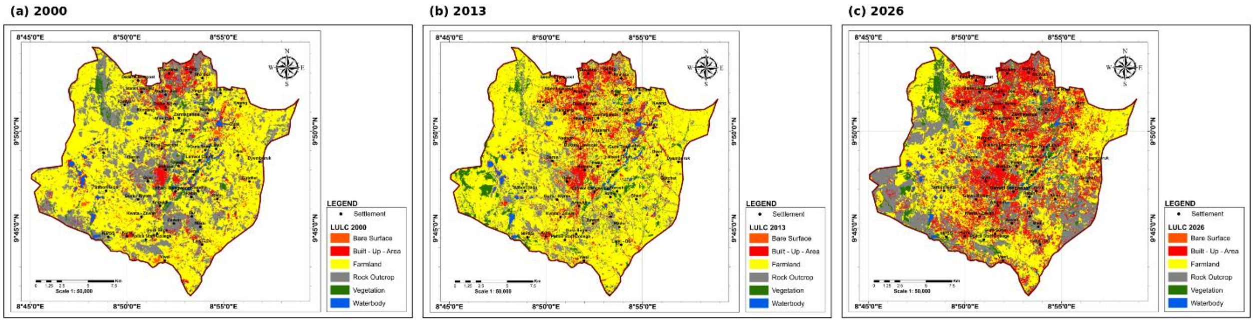

Figure 2. Classified Landcover for 2000, 2013 and 2026.

Vegetation increased from 8.84 to 17.75Km², while mapped bare surface declined from 6.11 to 2.27Km². These endpoint changes cannot be interpreted as equivalent ecological recovery because rock outcrop declined sharply in 2013 and then returned to 96.57Km² by 2026, while the transition matrix records large exchanges among farmland, exposed rocky substrate and built-up land. The endpoint composition therefore reflects a more heterogeneous and reworked landscape rather than a uniform reduction in disturbance.

3.2 Transition Matrix and Persistence

The exact 2000-2026 cross-tabulation shows that 169.0047Km² of the mapped landscape remained on the matrix diagonal. This represents 50.35% of the 335.6622Km² analytical extent, meaning that almost half of the landscape changed mapped class at least once between the two endpoints. Farmland accounted for the largest persistent area at 106.30Km², but it was also the principal source of new built-up land and rock outcrop/exposed rocky substrate.

Table 3. Landcover Transition Matrix, 2000 – 2026 (Km²).

2000 class → 2026 class	Built-up	Farmland	Vegetation	Waterbody	Bare surface	Rock outcrop	Total
Built-up area	12.23	2.11	0.18	0.44	0.19	3.85	**19.00**
Farmland	42.73	106.30	4.27	0.60	1.11	47.99	**203.00**
Vegetation	0.59	1.82	4.51	0.01	0.01	1.90	**8.84**
Waterbody	0.26	0.27	0.15	3.30	0.07	0.38	**4.43**
Bare surface	1.27	3.48	0.04	0.19	0.67	0.45	**6.11**
Rock outcrop	21.44	21.87	8.60	0.15	0.22	42.00	**94.29**
Total	**78.52**	**135.86**	**17.75**	**4.70**	**2.27**	**96.57**	**335.66**

The two largest off-diagonal transitions originated from farmland: 47.9880Km² moved to rock outcrop/exposed rocky substrate and 42.7293Km² moved to built-up land. Rock outcrop also supplied 21.4380Km² to built-up land and 21.8691Km² to farmland. These reciprocal exchanges are critical. They show that the small net increase in rock outcrop (+2.28Km²) conceals more than 100Km² of gross turnover involving that class, while the bare-surface decline cannot be equated with rehabilitation because much disturbed land shifted to other mapped sites.

Table 4. Persistence, Gross Loss, Gross Gain and Net Change Derived from the Full-Period Transition Matrix.

Class	Persistent area (Km²)	Persistence (%)	Gross loss (Km²)	Gross gain (Km²)	Net change (Km²)
Built-up area	12.23	64.36	6.77	66.29	+59.52
Farmland	106.30	52.36	96.70	29.56	-67.14
Vegetation	4.51	50.98	4.33	13.25	+8.92
Waterbody	3.30	74.41	1.13	1.40	+0.27
Bare surface	0.67	11.01	5.44	1.59	-3.84
Rock outcrop	42.00	44.55	52.28	54.57	+2.28

The gross-change diagnostics reveal the instability hidden by net statistics. Bare surface retained only 11.01% of its 2000 area, whereas waterbody had the highest class-specific persistence at 74.41%. Rock outcrop retained 44.55% of its 2000 area but experienced 52.28Km² of gross loss and 54.57Km² of gross gain. Thus, the apparent endpoint stability of rock outcrop is the net result of extensive spatial exchange rather than persistence of the same rocky surfaces. Because classification uncertainty may be greatest between farmland, bare surface and rock outcrop, these transition quantities must be interpreted together with the final accuracy assessment.

3.3 Mining Locations and Persistent Mining-Pond Corridors

Forty-six mining locations were mapped within the study area. The eastern and north-eastern cluster includes Gold and Base, Kwang, Dura, Latya, Dwei, Dyemburuk and Gutchet. Central concentrations occur around Gura Topp, Lahwol Chom, Fwati, Jerek, Koroshi, Rabin and Shen. The western and south-western sector is distinct because mining sites are accompanied by extensive clusters of water-filled excavations around Gero, Sabon Gida, Kuru, Gura Riyom, Kwata Zawan and Gura Suga. Many mapped ponds lie close to streams and low-lying drainage, consistent with the capture of rainfall, runoff and possibly shallow groundwater by excavated depressions.

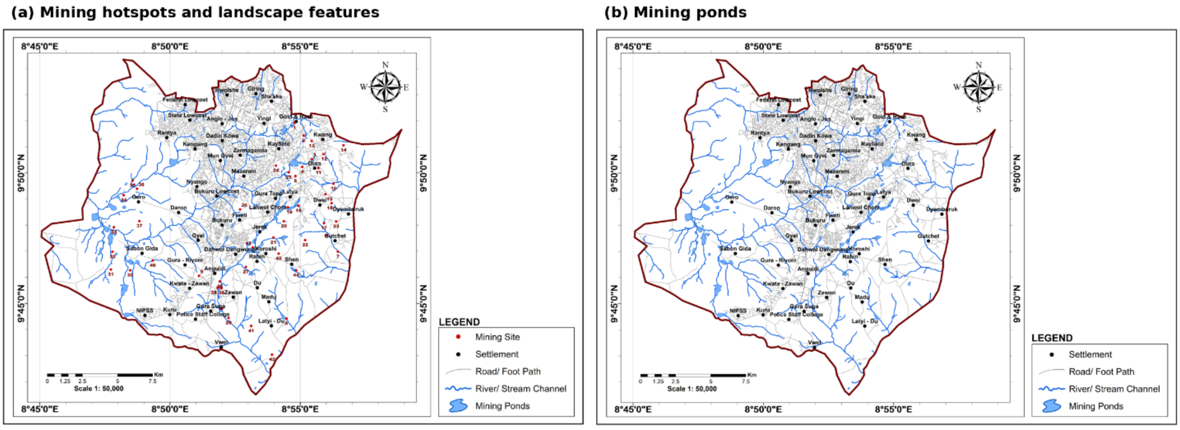

Figure 3. Spatial Distribution of Mapped Mining Locations, Landscape Features and Mining Ponds.

NDWI patterns reinforce the interpretation of a persistent western/ south-western pond corridor. Positive wetness signatures were already present in this belt in 2000, strengthened in 2013 and remained concentrated in the same broad zone in 2026. The evidence therefore supports persistence of a ponded mining-drainage landscape across the benchmark dates. It does not establish that every individual pond retained water continuously for 26 years, and it does not provide evidence of chemical contamination.

3.4 Spectral Evidence of Vegetation Response, Surface Exposure and Water

At the 2000 baseline, relatively stronger NDVI responses occurred in western and north-western locations, while low-NDVI surfaces were prominent along central settlement and disturbed corridors. BSI showed strong exposed-surface responses across northern, north-eastern, eastern and central locations. NDWI displayed distinct wetness signatures in the western and south-western mining belt, especially around Gero, Sabon Gida, NIPSS, Kuru, Gura Riyom, Kwata Zawan and Gura Suga. By 2013, stronger vegetation responses had developed in parts of the west and north-west, while exposed surfaces remained visible around the eastern mining corridor. In 2026, the overall pattern remained spatially heterogeneous, with vegetated patches, exposed/rocky surfaces, settlements and ponded excavation coexisting.

Table 5. Spectral-Index Extrema for NDVI, BSI and NDWI for the study Area.

Index	2000 Min/ Max	2013 Min/ Max	2026 Min/ Max	Interpretive Use
NDVI	-0.4831 / 0.3393	-0.2874 / 0.4320	-0.2764 / 0.4368	Spatial vegetation-response extremes only
BSI	-0.0986 / 0.5618	-0.1463 / 0.2248	-0.1512 / 0.2306	Exposed-surface extremes; not exposed area
NDWI	-0.3391 / 0.1895	-0.4065 / 0.2804	-0.4223 / 0.2868	Water/ moisture extremes; not water-area change

The rise in the maximum NDVI from 0.3393 in 2000 to 0.4368 in 2026 indicates that the strongest vegetated pixels expressed a higher spectral response at the later dates. It does not demonstrate landscape-wide ecological recovery because maxima describe only extreme pixels and may represent crops, grasses, shrubs or secondary colonisation. Similarly, the decline in maximum BSI after 2000 indicates a reduction in the strongest exposed-surface response, not a 60% reduction in degraded area. In mining zones, pond water can suppress BSI within excavation voids while exposed banks and spoil remain adjacent.

NDWI maxima increased from 0.1895 to 0.2804 and 0.2868 across the three dates, while minima became more negative. The widening spectral range is consistent with stronger separation between wet and dry surfaces. The most defensible evidence is spatial: positive signatures repeatedly overlap the western and south-western mining-pond corridor. A quantitative statement about change in total pond or open-water area would require one common, validated water threshold or object-based pond delineation applied consistently across all dates.

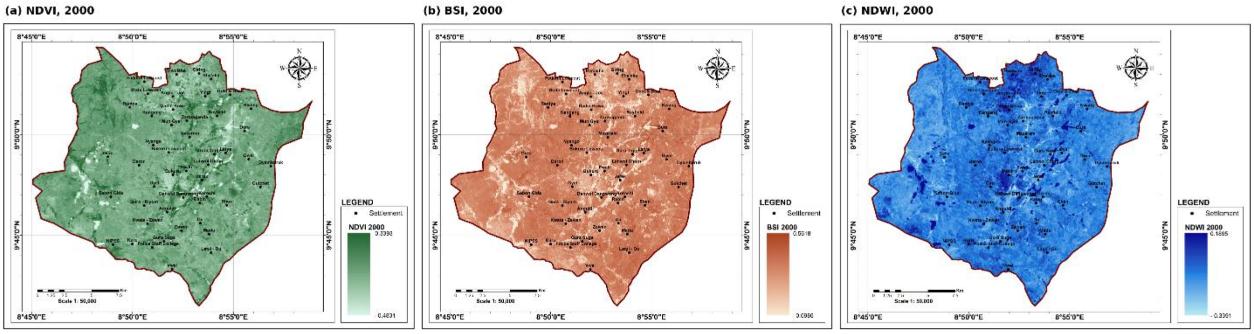

Figure 4. Spatial pattern of NDVI, BSI and NDWI in 2000.

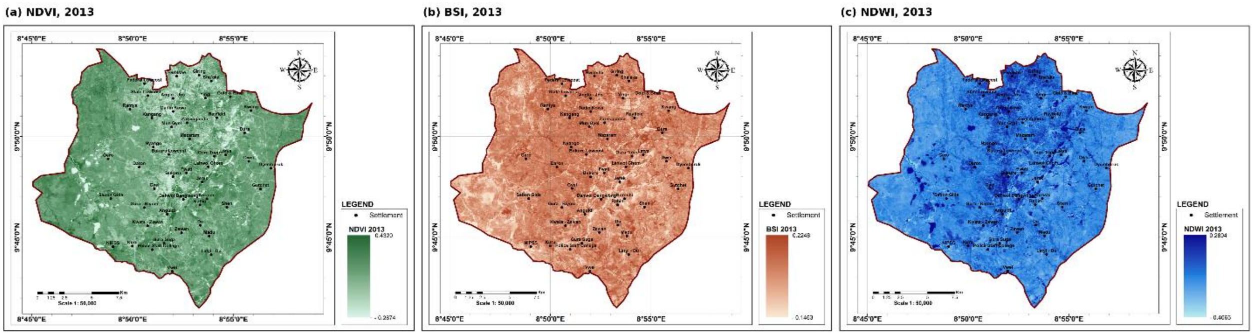

Figure 5. Spatial pattern of NDVI, BSI and NDWI in 2013.

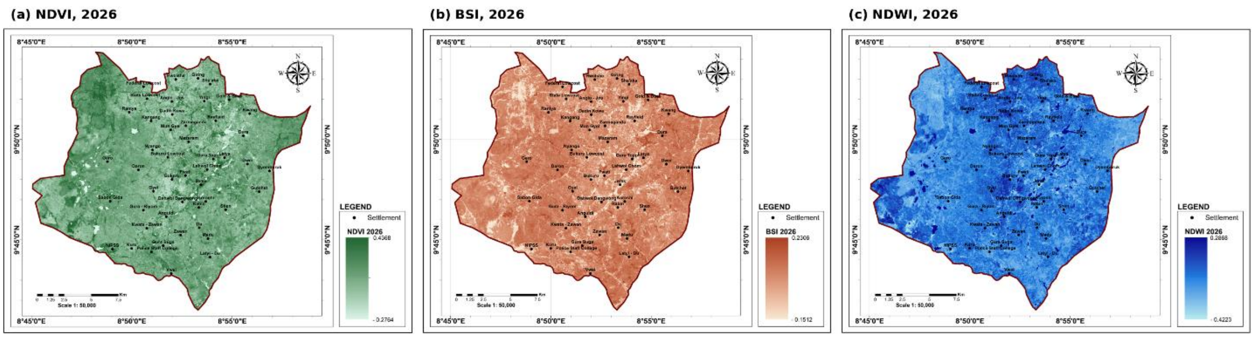

Figure 6. Spatial pattern of NDVI, BSI and NDWI in 2026.

IV. Discussion

In this study, the clearest long-term reconfiguration is the contraction of farmland alongside rapid built-up expansion. Farmland lost 67.14Km² while built-up land gained 59.52Km², and the transition matrix shows that 42.73Km² of 2000 farmland became built-up by 2026. This direct source-to-destination evidence is stronger than comparing class totals alone. It is consistent with earlier research in Jos South L.G.A. that documented encroachment on arable land from urbanisation and related development pressures (Musa et al., 2015).

Comparable mining regions in Ghana also show that mining and settlement growth can fragment agricultural landscapes and intensify competition for productive land (Aggrey et al., 2021; Mensah et al., 2025).

The magnitude and spatial distribution of built-up growth along the Jos-Bukuru metropolitan corridor cannot reasonably be assigned to mining alone. Population growth, residential demand, road development and commercial expansion are major alternative drivers. Mining can interact with these processes by opening access, attracting labour and stimulating local markets, but the evidence supports a multi-driver landscape rather than a single-cause narrative. This distinction matters for policy because reclamation of mine sites will not reverse farmland loss caused primarily by urban development.

Bare Surface had only 11.01% persistence, while farmland and rock outcrop experienced large reciprocal exchanges. A disturbed mining surface can move spectrally and categorically from bare soil to exposed rock, water-filled excavation, settlement or secondary vegetation without restoration of pre-disturbance soil structure, hydrology or ecological function. Mining-landscape studies elsewhere have likewise shown that Landcover Classes can reorganise while degradation, fragmentation and water disturbance persist (Gbedzi et al., 2022; Kumi et al., 2023; Bansah et al., 2024).

Rock Outcrop result was only 2.28Km², yet gross losses and gains exceeded 52Km² in each direction. Some of this turnover may represent genuine physical reworking of exposed rocky terrain, mine excavation, vegetation or cultivation over thin rocky substrate, and settlement growth.

Vegetation area approximately doubled from the low 2000 baseline and the strongest NDVI pixels had higher values in 2013 and 2026. These findings are compatible with local secondary vegetation growth, cultivation, revegetation of abandoned surfaces or differences in seasonal vegetation condition. They do not establish restoration of pre-mining ecological function. Secondary grasses and shrubs can produce strong NDVI values even where soil profiles, hydrology and habitat structure remain altered. Ogunro and Owolabi (2023) similarly reported vegetation improvement in parts of the Jos landscape while concluding that mining and land-use pressure persisted. The coexistence of stronger vegetation response, extensive settlement expansion, exposed rocky surfaces and mining ponds supports a mosaic interpretation rather than a uniform recovery trajectory.

The western and south-western pond belt is one of the most distinctive mining legacies in the study area. Mapped pond clusters occur around Gero, Sabon Gida, Kuru, Gura Riyom, Kwata Zawan and Gura Suga, and recurrent NDWI responses occupy the same broad corridor at all three benchmark dates. Many ponds are spatially connected to drainage channels, which provides a plausible mechanism for repeated water retention in excavation depressions. Similar mining landscapes in West Africa demonstrate that excavation and disturbed soils can alter runoff pathways, sediment delivery and the distribution of surface water (Gbedzi et al., 2022; Kumi et al., 2023).

The findings in this favour a transition-aware monitoring framework. Regulatory inventories should distinguish active excavation, abandoned pits, water-filled excavations, spoil surfaces, exposed rock, reclaimed land and settlement rather than collapsing them into a single “degraded” class. Annual or biennial Earth-observation updates, supported by field or drone verification, would allow detection of new excavation fronts, pond formation, infilling, revegetation and urban encroachment.

Recent remote-sensing reviews of ASM similarly argue for repeated observations and integration with local or field information to improve mapping reliability (Nursamsi et al., 2024). A 2026 Ghanaian study using digitised mine sites and LULC analysis also illustrates the value of explicitly mapping mine expansion rather than inferring mining solely from broad Landcover Classes (Tetteh et al., 2026).

V. Conclusion

The mapped portion of Jos South underwent substantial landscape reconfiguration between 2000 and 2026. Built-up land increased by 59.52Km² while farmland declined by 67.14Km², and only 50.35% of the landscape retained the same mapped class. The full transition matrix shows that farmland was the dominant source of both new built-up land and rock outcrop/exposed rocky substrate, while rock outcrop itself experienced extensive gross exchange that is hidden by its small net change. These findings demonstrate why endpoint class totals alone are inadequate for interpreting mining-affected landscapes.

The spectral and feature evidence adds a second layer of interpretation. Vegetation response strengthened in some locations and the most extreme bare-surface response declined, yet exposed and rocky surfaces remained spatially associated with mining and settlement corridors. Recurrent wetness signatures and mapped ponds define a persistent mining-pond corridor in the western and south-western drainage belt. The evidence therefore supports neither uniform degradation nor broad ecological recovery. Instead, the study area is a heterogeneous mining-influenced landscape in which extraction legacies, urban expansion, agricultural contraction, secondary vegetation and hydrological modification coexist.

For Jos South, reclamation priorities should focus on locations where excavation pits, unstable exposed surfaces, drainage lines and settlements intersect. Landuse planning should separately address the conversion of farmland to urban uses because mine rehabilitation alone cannot resolve metropolitan land competition. The full transition matrix can also serve as a baseline for future intensity analysis, allowing researchers to test whether particular gains, losses and transitions are systematically active across successive intervals rather than merely large in absolute area.

References

[1]. Aggrey, J. J., Ros-Tonen, M. A. F., & Asubonteng, K. O. (2021). Using participatory spatial tools to unravel community perceptions of land-use dynamics in a mine-expanding landscape in Ghana. Environmental Management, 68, 720-737. https://doi.org/10.1007/s00267-021-01494-7

[2]. Aldwaik, S. Z., & Pontius, R. G., Jr. (2012). Intensity analysis to unify measurements of size and stationarity of land changes by interval, category, and transition. Landscape and Urban Planning, 106(1), 103-114. https://doi.org/10.1016/j.landurbplan.2012.02.010

[3]. Bala, A., Garba, S., Adewuyi, T., & Youngu, T. (2021). Geospatial analyses of mining-induced land degradation sites in Jos South Local Government Area, Plateau State-Nigeria. FIG Proceedings, 2021, 1-15.

[4]. Bansah, K. J., Acquah, P. J., & Boafo, A. (2024). Land, water, and forest degradation in artisanal and small-scale mining: Implications for environmental sustainability and community wellbeing. Resources Policy, 90, 104795. https://doi.org/10.1016/j.resourpol.2024.104795

[5]. Gbedzi, D. D., Ofosu, E. A., Mortey, E. M., Obiri-Yeboah, A., Nyantakyi, E. K., Siabi, E. K., Abdallah, F., Domfeh, M. K., & Amankwah-Minkah, A. (2022). Impact of mining on land use land cover change and water quality in the Asutifi North District of Ghana, West Africa. Environmental Challenges, 6, 100441. https://doi.org/10.1016/j.envc.2022.100441

[6]. Kumi, S., Adu-Poku, D., & Attiogbe, F. (2023). Dynamics of land cover changes and condition of soil and surface water quality in a mining-altered landscape, Ghana. Heliyon, 9(7), e17859. https://doi.org/10.1016/j.heliyon.2023.e17859

[7]. Mensah, S. K., Nyantakyi, E. K., Mensah, G. S., Siabi, E. K., Ackerson, N. O. B., Antwi-Agyei, P., Donkor, P., & Siabi, S. E. (2025). Assessing the impact of small-scale mining activities on land use land cover and the sustainability of mining practices in Ghana: A case of the Atiwa East district. Resources Policy, 109, 105719. https://doi.org/10.1016/j.resourpol.2025.105719

[8]. Musa, H. D., & Jiya, S. N. (2011). An assessment of mining activities impact on vegetation in Bukuru, Jos Plateau State Nigeria using Normalized Differential Vegetation Index (NDVI). Journal of Sustainable Development, 4(6), 150-162. https://doi.org/10.5539/jsd.v4n6p150

[9]. Musa, I. T., Owa, O., & Lekwot, V. E. (2015). Assessment of arable land loss due to urbanization using remote sensing and GIS: A study of Jos South Local Government Area of Plateau State, Nigeria. American Based Research Journal, 4, 1-15.

[10]. Ndace, J. S., & Danladi, M. H. (2012). Impacts of derived tin mining activities on land use/land cover in Bukuru, Plateau State, Nigeria. Journal of Sustainable Development, 5(5), 90-100. https://doi.org/10.5539/jsd.v5n5p90

[11]. Ncube-Phiri, S., Ncube, A., Mucherera, B., & Ncube, M. (2015). Artisanal small-scale mining: Potential ecological disaster in Mzingwane District, Zimbabwe. Jàmbá: Journal of Disaster Risk Studies, 7(1), 158. https://doi.org/10.4102/jamba.v7i1.158

[12]. Nursamsi, I., Phinn, S. R., Levin, N., Luskin, M. S., & Sonter, L. J. (2024). Remote sensing of artisanal and small-scale mining: A review of scalable mapping approaches. Science of the Total Environment, 951, 175761. https://doi.org/10.1016/j.scitotenv.2024.175761

[13]. Ogunro, O. T., & Owolabi, A. O. (2023). Assessment of the sustainability of LULCs due to artisanal mining in Jos area, Nigeria. Environmental Science and Pollution Research, 30(13), 36502-36520. https://doi.org/10.1007/s11356-022-24143-w

[14]. Olofsson, P., Foody, G. M., Herold, M., Stehman, S. V., Woodcock, C. E., & Wulder, M. A. (2014). Good practices for estimating area and assessing accuracy of land change. Remote Sensing of Environment, 148, 42-57. https://doi.org/10.1016/j.rse.2014.02.015

[15]. Pontius, R. G., Jr., & Millones, M. (2011). Death to Kappa: Birth of quantity disagreement and allocation disagreement for accuracy assessment. International Journal of Remote Sensing, 32(15), 4407-4429. https://doi.org/10.1080/01431161.2011.552923

[16]. Tetteh, A. T., Yevugah, L. L., & Moomen, A.-W. (2026). Mapping the expansion of artisanal and large-scale mining in Birim North District, Ghana using land use land cover change and digitized mine sites. Regional Science Policy & Practice, 18(8), 100325. https://doi.org/10.1016/j.rspp.2026.100325. (8)